Drift Compression of an Intense Neutralized Ion Beam

P. K. Roy,[1] S. S. Yu,[1] E. Henestroza,[1] A. Anders,[1] F. M. Bieniosek,[1] J. Coleman,[1] S. Eylon,[1] W. G. Greenway,[1] M. Leitner,[1] B. G. Logan,[1] W. L. Waldron,[1] D. R. Welch,[2] C. Thoma,[2] A. B. Sefkow,[3] E. P. Gilson,[3] P. C. Efthimion,[3] and R. C. Davidson[3]

[1]*Lawrence Berkeley National Laboratory, 1 Cyclotron Road, Berkeley, California, 94720, USA*
[2]*ATK Mission Research, Albuquerque, New Mexico 87110-3946, USA*
[3]*Princeton Plasma Physics Laboratory, Princeton, New Jersey 08543-0451, USA*

(Received 9 September 2005; published 29 November 2005)

Longitudinal compression of a velocity-tailored, intense neutralized K^+ beam at 300 keV, 25 mA has been demonstrated. The compression takes place in a 1–2 m drift section filled with plasma to provide space-charge neutralization. An induction cell produces a head-to-tail velocity ramp that longitudinally compresses the neutralized beam, enhancing the beam peak current by a factor of 50 and producing a pulse duration of about 3 ns. This measurement has been confirmed independently with two different diagnostic systems.

DOI: 10.1103/PhysRevLett.95.234801 PACS numbers: 41.85.Ct

To create high energy density matter and fusion conditions, high power drivers, such as lasers, ion beams, and x-ray drivers, are needed to heat targets with pulses short compared to hydromotion. Both high energy density physics and ion-driven inertial fusion require the simultaneous transverse and longitudinal compression of an ion beam to achieve high intensities.

Longitudinal compression of space-charge-dominated beams has been studied extensively in theory and simulations [1–6]. The compression is initiated by imposing a linear head-to-tail velocity tilt to a drifting beam. Longitudinal space-charge forces limit the beam compression ratio, the ratio of the initial to final current, to about ten in most applications. An experiment with fivefold compression has been reported [7]. Recent theoretical models and simulations predict that much higher compression ratios (≤ 100) can be achieved if beam compression takes place in a plasma-filled drift region in which the space-charge forces of the ion beam are neutralized [8,9]. If the compressed pulse length t_p is dominated by the longitudinal beam temperature T_l, t_p is approximately given by

$$t_p = \frac{L}{v_l^2}\sqrt{\frac{2kT_l}{M}}, \tag{1}$$

where v_l, L, M, and k are the mean longitudinal beam velocity, drift length, mass of ion, and Boltzmann constant, respectively. In this Letter, temporal bunch compression of an intense ion beam is demonstrated using a neutralized drift section and a tilted velocity distribution.

Figure 1 shows a schematic of the neutralized drift compression experimental (NDCX) setup. The NDCX experiment uses the same front end as the earlier neutralized transport experiments (NTX) [10–15]. It consists of a 300 keV, 25-milliamp K^+ beam from an alumino silicate source powered by a Marx generator. The beam produced from the source has a 6 μs flattop. Four pulsed quadrupoles magnets used in NTX to control the beam envelope (beam radius and convergence angle) are retained for the present experiments on NDCX.

To provide the head-to-tail velocity tilt, an induction module with a variable voltage waveform is placed immediately downstream of the last quadrupole magnet. The induction cell consists of 14 independently driven magnetic cores in a pressurized gas (SF_6) region that is separated from the vacuum by a conventional high voltage insulator. The waveforms applied to the 14 cores inductively add at the acceleration gap. Each core is driven by a thyratron-switched modulator. Because the modulator for each core can be designed to produce different waveforms and can be triggered independently, a variety of waveforms can be produced at the acceleration gap using the 14 discrete building blocks. The induction tilt voltage ''carves'' out a ~300 ns segment of the flattop which compresses longitudinally as it drifts through a one-meter long plasma column.

The plasma column is formed by two pulsed aluminum cathodic arc sources [16] located at the downstream end. Each source is equipped with a 45° open-architecture macroparticle filter providing a flow of fully ionized alu-

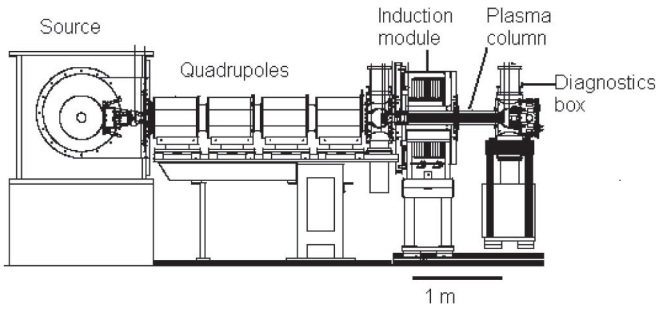

FIG. 1. Schematic of the NDCX experimental setup.

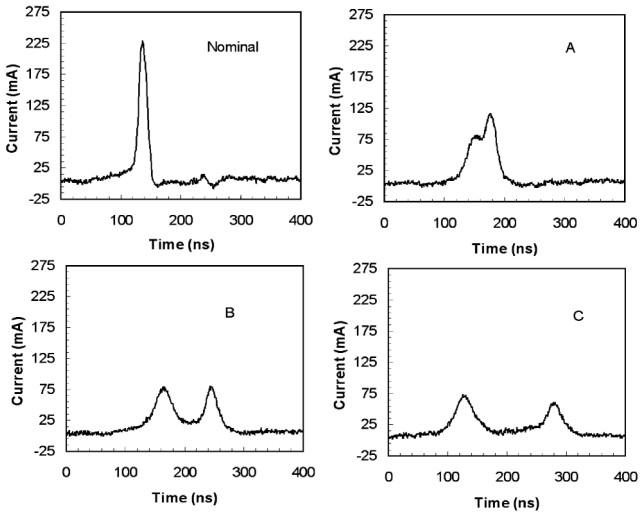

FIG. 2. Neutralized drift-compressed beam current with the voltage waveforms in Fig. 3.

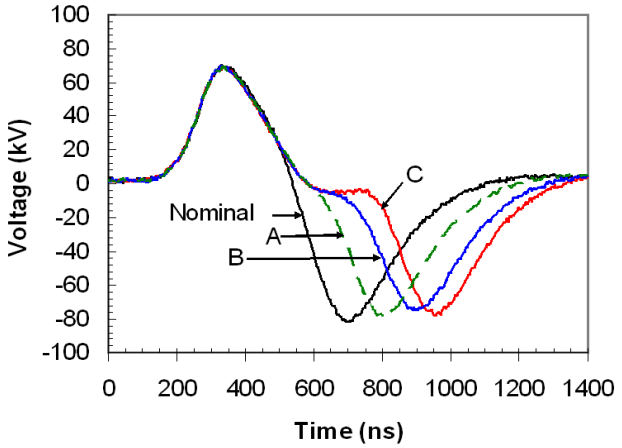

FIG. 3 (color online). Induction module voltage waveforms produced by varying the timing of the modulators.

minum plasma [17]. The two plasma flows are pointed at an angle of 45° towards the solenoidal column (~1 kG, 7.6 cm diameter, and 1 m long). In most of the operating regimes, the plasma density ($\sim 5 \times 10^{10}$ cm^{-3}) is at least a factor of 10 higher than the beam density. At the upstream end of the column, we have introduced a "plasma stopper" consisting of two opposing dipoles of ~1 kG each, which inhibit the motion of plasma upstream into the induction gap and quadrupole focusing sections. A diagnostic box is located at the downstream end of the plasma column. The final compressed beam is measured in the downstream diagnostic box.

A phototube diagnostic [18] is used to measure beam pulse compression with and without neutralization by background plasma. The optical system is based on a Hamamatsu phototube with fast (sub-ns) response which is coupled to a 500 MHz oscilloscope. The beam pulse is measured by using the phototube to collect the optical photon flux from an aluminum oxide scintillator placed in the path of the beam. The time response of the scintillator is fast enough to make measurements on a nanosecond time scale. The background plasma light is blocked from entering the phototube by an electro-optic gated shutter (Displaytech) that opens just before the beam pulse arrives at the scintillator. The scintillator itself is not sensitive to low-energy plasma electrons. As a result, we have been able to obtain beam pulse compression data with minimal interference from the neutralizing plasma.

A second diagnostic, a Faraday cup, is used for measurements of the current. The Faraday cup is specially designed [19] to function in a plasma environment. It consists of hole plates with hole sizes comparable to the Debye length, in order to prevent plasma from entering into the cup. The cup geometry and external circuitry are optimized to assure fast time response (<3 ns).

When the tilt voltage waveform is turned on, beam bunching is observed in the downstream diagnostic box. The degree of bunching, as well as the pulse shape, shown in Fig. 2, is clearly correlated with the voltage waveform, shown in Fig. 3. Theory specifies the ideal voltage waveform required to produce an exactly linear (versus z) velocity ramp [8,9]. The induction module voltage waveform is optimized to obtain a rather close approximation to the ideal waveform as shown in Fig. 4.

For a given voltage waveform, the position of maximal compression is changed as the beam energy is varied. A scan in beam energy demonstrates this behavior and is shown in Fig. 5. The maximum compression is observed by fine-tuning the beam energy to match the voltage waveform and precisely position the longitudinal focal point at the diagnostic location. This is shown in Fig. 6. The ~50 fold compression ratio [see Fig. 6(b)] is obtained by taking the ratio of the signal with tilt voltage on (with compression) to the signal with tilt voltage off (without compression) [see Fig. 6(a)]. A similar result is measured with the Faraday cup [see Fig. 6(c)]. LSP [20] calculations under these experimental conditions predict a peak compression ratio of 60 [see Fig. 6(d)].

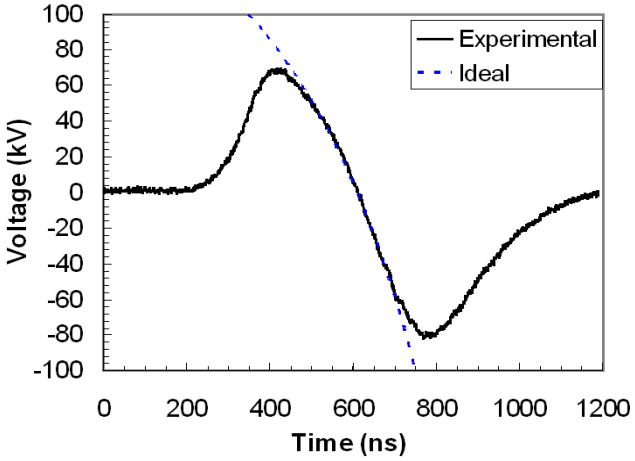

FIG. 4 (color online). Experimentally optimized and ideal induction module voltage waveforms.

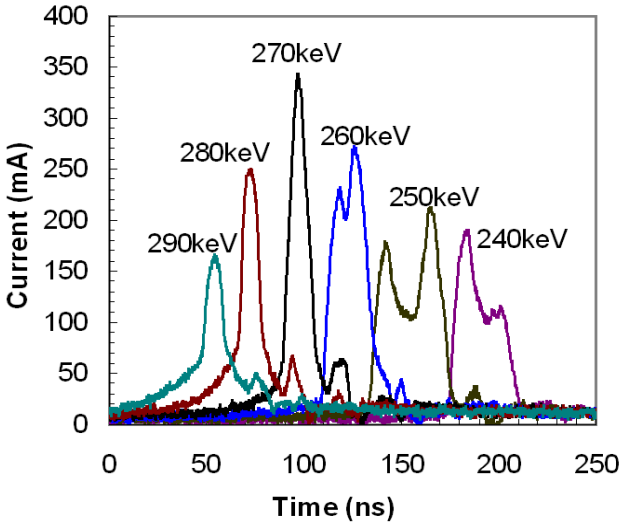

FIG. 5 (color online). Compressed beam current pulses using a nominal tilt core voltage waveform as the beam energy is varied.

The strong effects of neutralization are evident by comparing the compression ratio with the plasma turned on and off. Figure 7 shows that the peak current is significantly reduced when the plasma is turned off. LSP simulations under similar conditions show qualitatively similar results.

Theory predicts that the nature of beam compression is strongly dependent on the drift length [8]. As the length is increased, the compression is more sensitive to the degree of neutralization. It is also more sensitive to the intrinsic longitudinal temperature of the ion beam. Finally, if there

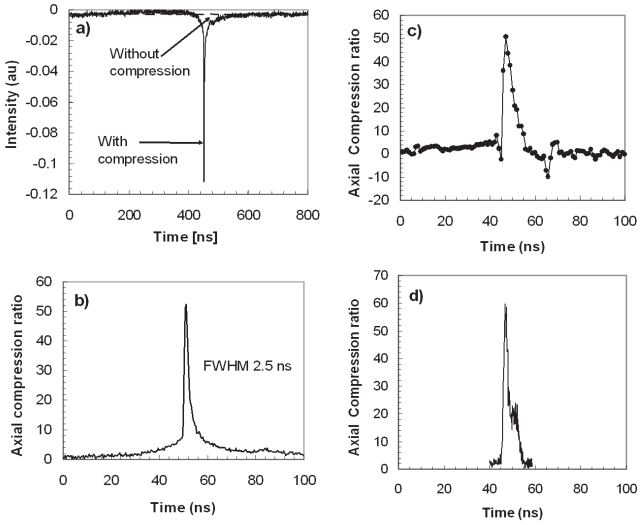

FIG. 6. (a) Measurements of beam signal using the phototube diagnostic for neutralized noncompressed, and neutralized compressed beams, (b) compression ratio obtained from the measurements using the phototube, (c) compression ratio obtained from measurements using the Faraday cup, and (d) LSP (an electromagnetic particle-in-cell code) simulation for axial compression ratio under the experimental conditions.

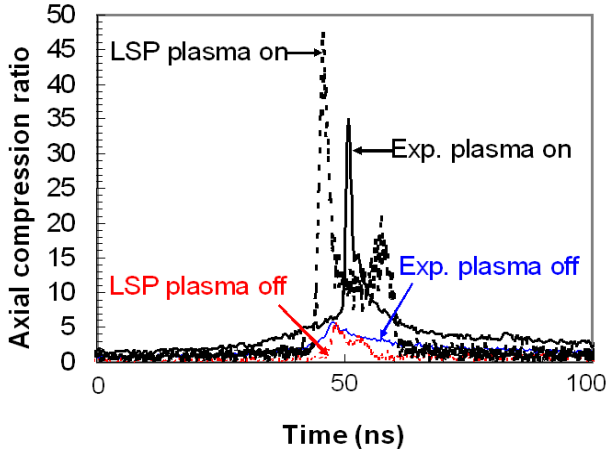

FIG. 7 (color online). Experimental data and LSP simulation of beam compression with neutralization (plasma source on) and without neutralization (plasma source off).

are any instabilities, e.g., two-stream, they may become evident with longer drift lengths.

For the above reasons, we have performed additional experiments with the drift length with plasma extended to two meters. We are able to recover the 50-fold compression in the 2 m experiment as shown in Fig. 8. The corresponding LSP simulation is also shown.

On the basis of this two-meter experiment we conclude that: (1) the degree of charge neutralization is sufficient to achieve 50-fold longitudinal compression while avoiding space-charge blowup of the beam for the experimental configuration investigated; (2) the intrinsic longitudinal temperature is <1 eV; and (3) no collective instabilities have been observed.

Transverse as well as longitudinal compression is required to achieve the high intensity required for high energy density physics and fusion, as mentioned earlier. Simulations indicate that small spot sizes, required for

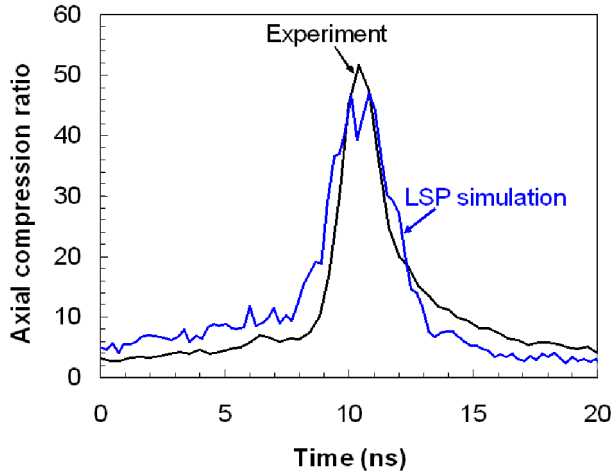

FIG. 8 (color online). Comparison of beam compression between experiment and LSP simulation for the 2 m long plasma column.

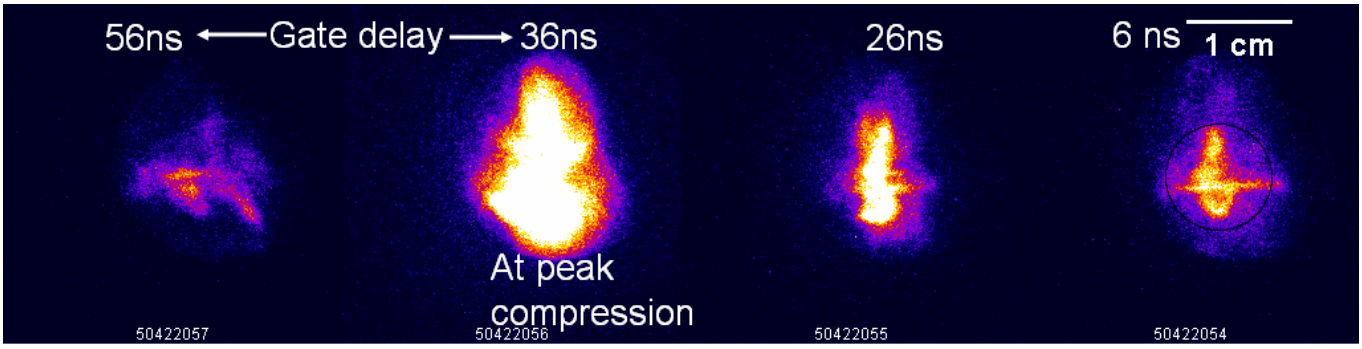

FIG. 9 (color online). Transverse profiles of neutralized compressed beam using a gated camera.

fusion targets [21,22], could be achieved with plasma neutralization [20,23]. We have previously studied [10–13] the effects of plasma neutralization. This scaled experiment, the neutralized transport experiment (NTX), demonstrated that an un-neutralized beam of several centimeter radius can be compressed transversely to ~1 mm radius when charge neutralization by background plasma electrons is provided, in quantitative agreement with the simulation [14,15].

In NDCX, optical imaging has been deployed to measure the transverse beam size as a function of time during longitudinal compression. We are able to measure the images with a 1 ns time resolution. It is interesting to observe that the transverse spot size is larger at the point of maximal compression, as shown in Fig. 9. This feature is due to time-dependent defocusing effects occurring at the induction gap. The theory and simulations of this effect will be reported elsewhere. We are just beginning to explore combined transverse and longitudinal compression.

This Research was supported by the U.S. Department of Energy under Contract No. DE-AC02-05CH11231 with the Lawrence Berkeley National Laboratory, and Contract No. DE-AC02-76CH03073 with Princeton Plasma Physics Laboratory. We thank Dr. A. Friedman, Dr. J. Barnard, Dr. C. Celata, Dr. I. Kaganovich, Dr. E. Lee, Dr. P. Seidl, and Dr. W. M. Sharp for useful discussions and comments. Thanks also to Mr. D. Baca and Mr. D. L. Vanecek for useful technical assistance.

[1] D. D.-M. Ho *et al.*, Part. Accel. **35**, 15 (1991).
[2] T. Kikuchi *et al.*, Phys. Plasmas **9**, 3476 (2002).
[3] M. J. L. de Hoon *et al.*, Phys. Plasmas **10**, 855 (2003).
[4] H. Qin *et al.*, Phys. Rev. ST Accel. Beams **7**, 104201 (2004).
[5] R. C. Davidson and H. Qin, Phys. Rev. ST Accel. Beams **8**, 064201 (2005).
[6] W. M. Sharp *et al.*, Nucl. Instrum. Methods Phys. Res., Sect. A **544**, 398 (2005).
[7] W. M. Fawley *et al.*, Phys. Plasmas **4**, 880 (1997).
[8] D. R. Welch *et al.*, Nucl. Instrum. Methods Phys. Res., Sect. A **544**, 236 (2005).
[9] C. Thoma *et al.*, Proceedings of the 2005 Particle Accelerator Conference (IEEE, New York, to be published).
[10] S. S. Yu *et al.*, in *Proceedings of the 2003 Particle Accelerator Conference*, edited by J. Chew (IEEE, New York, 2003), p. 98.
[11] E. Henestroza *et al.*, Phys. Rev. ST Accel. Beams **7**, 083501 (2004).
[12] P. K. Roy *et al.*, Phys. Plasmas **11**, 2890 (2004).
[13] B. G. Logan *et al.*, Nucl. Fusion **45**, 131 (2005).
[14] C. Thoma *et al.*, Phys. Plasmas **12**, 043102 (2005).
[15] P. K. Roy *et al.*, Nucl. Instrum. Methods Phys. Res., Sect. A **544**, 225 (2005).
[16] A. Anders and G. Y. Yushkov, J. Appl. Phys. **91**, 4824 (2002).
[17] A. Anders and R. A. MacGill, Surf. Coat. Technol. **133-134**, 96 (2000).
[18] F. M. Bieniosek *et al.*, Nucl. Instrum. Methods Phys. Res., Sect. A **544**, 268 (2005).
[19] A. Sefkow *et al.*, Proceedings of the 2005 Particle Accelerator Conference (IEEE, New York, to be published).
[20] D. R. Welch *et al.*, Nucl. Instrum. Methods Phys. Res., Sect. A **464**, 134 (2001).
[21] S. S. Yu *et al.*, Nucl. Instrum. Methods Phys. Res., Sect. A **544**, 294 (2005).
[22] W. M. Sharp *et al.*, Fusion Sci. Technol. **43**, 393 (2003).
[23] W. M. Sharp *et al.*, Nucl. Fusion **44**, S221 (2004).